The impact of vertical-axis rotations on shortening estimates

Aviva J. Sussman[1,*], Emilio L. Pueyo[2,*], Clement G. Chase[3,*], Gautam Mitra[4,*], and Arlo B. Weil[5,*]
[1]EARTH AND ENVIRONMENTAL SCIENCES, MS-D443, LOS ALAMOS NATIONAL LABORATORY, LOS ALAMOS, NEW MEXICO 87545, USA
[2]INSTITUTO GEOLÓGICO Y MINERO DE ESPAÑA, UNIDAD DE ZARAGOZA, CALLE MANUEL LASALA 44, 9°, Z50006, SPAIN
[3]DEPARTMENT OF GEOSCIENCES, UNIVERSITY OF ARIZONA, TUCSON, ARIZONA 82571, USA
[4]DEPARTMENT OF EARTH AND ENVIRONMENTAL SCIENCES, UNIVERSITY OF ROCHESTER, ROCHESTER, NEW YORK 14627, USA
[5]DEPARTMENT OF GEOLOGY, BRYN MAWR COLLEGE, BRYN MAWR, PENNSYLVANIA 19010, USA

ABSTRACT

The total amount of deformation between two converging bodies is described by the three components of the displacement field: translation, rotation, and strain. Translations along faults and folding strain are the most common elements of the displacement field incorporated into estimates of tectonic shortening across orogenic systems. Determinations of vertical-axis rotations through paleomagnetic and structural analyses are keys for deciphering the rotational component of shortening within an orogenic system, and they can have a substantial effect on the amount of tectonic shortening in such systems. Accommodation structures observed in orogenic systems are typically noncoaxial and/or noncylindrical geometries (e.g., oblique and lateral ramps, superposed folding). These structures suggest that vertical-axis rotations have taken place, can aid in determining the relative timing of rotation with respect to translation, and may help constrain the location of the rotation axis. In this paper, we define the components of the total displacement field, describe the diagnostic and suggestive features associated with vertical-axis rotations, and apply trigonometric map-view calculations to estimate the amount of shortening contributed by such rotations. An error function relating shortening with vertical-axis rotation has been calculated and predicts values up to 50% for a 60° rotation if the rotation is not taken into account. Finally, we apply our approach to the Wyoming salient and show that previous estimates of shortening there may contain up to 14% error.

LITHOSPHERE; v. 4; no. 5; p. 383–394 | Published online 7 August 2012 doi: 10.1130/L177.1

INTRODUCTION

For an initial reference object, translation, rotation, and strain (distortion) all comprise the term "deformation" and together make up the total displacement field (Means, 1976; Cobbold, 1979), which represents the change in shape and position of a deformed object. Shape change (strain) can be achieved through simple shear, pure shear, and/or general shear, and a position change is achieved through translation and/or rotation (Fig. 1). While tectonic investigations have become increasingly concerned with three-dimensional transport and orogenic curvature, (e.g., see Weil and Sussman, 2003, and references therein; Soto et al., 2006; Weil et al., 2010), the most widely used tool to measure shortening in fold-and-thrust belts is the balanced cross section (e.g., Dahlstrom, 1969; Hossack, 1979), which assumes plane strain.

The most recent three-dimensional restoration methods (Gratier et al., 1991; Williams et al., 1997; Erickson et al., 2000; Rouby et al., 2000; Dunbar and Cook, 2003; Thibert et al., 2005; Muron et al., 2005; Moretti et al., 2005; Moretti, 2008; Guzofski et al., 2009) do not adequately consider vertical-axis rotations. Work by Pueyo et al. (2004), Oliva-Urcia and Pueyo (2007), and Arriagada et al. (2008) has attempted to quantify the magnitude and spatial distribution of vertical-axis rotations to achieve viable map-view restorations. Recently, Ramón et al. (2012) developed a restoration tool that incorporates paleomagnetic vectors to unfold surfaces in three dimensions. Here, we suggest an approach that incorporates all components of the total displacement field into shortening estimates. Although we emphasize paleomagnetic analysis as a primary method for determining the distribution, direction, and magnitude of rotations, since it provides absolute values for rotation (direction/sense and magnitude), we note that structural techniques, such as calcite twin analysis (e.g., Groshong, 1972), can also be used but are more limited in their ability to quantify magnitudes due to a lack of a stable reference frame. Finally, we present an example of the effects of vertical-axis rotations on shortening estimates from the Wyoming salient of the Sevier orogen in the western United States. This example is used to show the impact that vertical-axis rotations have on tectonic shortening estimates and, thus, the potential impact that vertical-axis rotations have on our understanding as to the structural evolution of contractional orogens.

*E-mails: spring@lanl.gov; unaim@igme.es; chase@geo.arizona.edu; gautam.mitra@rochester.edu; aweil@brynmawr.edu.

TOTAL DISPLACEMENT FIELD

Using Cartesian tensor notation, the displacement field for an orogen can be defined as: $\omega_i = X'_i - X_i$, where $X_i = X_1, X_2, X_3$ is the initial location of a point in the orogen and $X'_i = X'_1, X'_2, X'_3$ is the final location of the point (e.g., finite deformation of Ramsay, 1967). This notation becomes significantly more complicated when considering deformation of objects of dimension, such as lines, planes, and constant volumes. Whereas the deformation of a point can be described by a vector, the deformation of other objects, such as lines, planes, and constant volumes, requires elements of rotation, translation, and internal strain. For an individual point, ω_i represents the total translation. The displacement gradient, or incremental deformation tensor, is defined by D_{ij} with

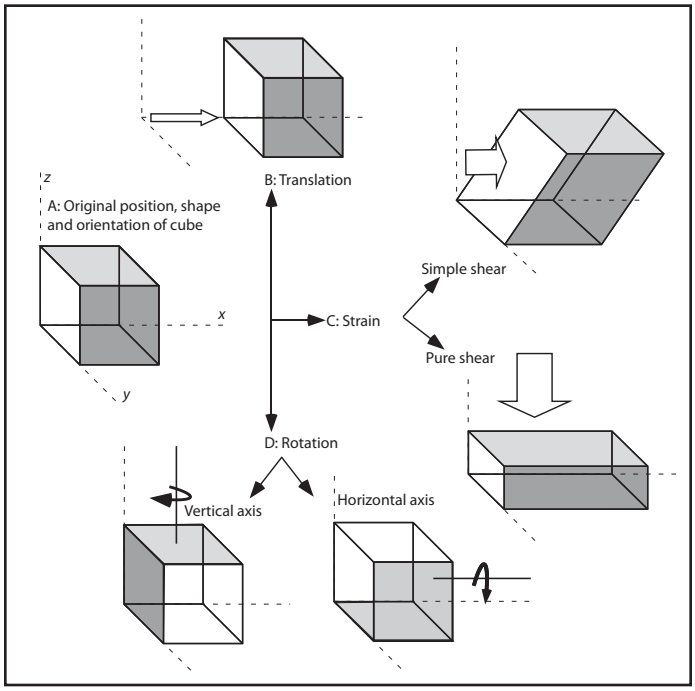

Figure 1. The three components of deformation: translation, strain, and rotation (Means, 1976) constitute the total displacement field for material moving within an orogenic system. (A) The original position, shape, and orientation of the cube with respect to a Cartesian coordinate frame. (B) New position of cube after translation along the *x*-axis. Translation in orogens may occur in any direction or combination of directions. (C) Strained cubes after having undergone pure or simple shear. Shape change may also take place by general shear. (D) Rotations occur about vertical, horizontal, or inclined (not pictured) axes.

$$D_{ij} = \partial\omega_i / \partial x_j$$

and can be decomposed into symmetric and antisymmetric components. The symmetric component is the strain tensor

$$\varepsilon_{ij} = \frac{1}{2}\left(\frac{\partial\omega_j}{\partial x_i} + \frac{\partial\omega_i}{\partial x_j}\right),$$

and the antisymmetric component is the rotation tensor

$$r_{ij} = \frac{1}{2}\left(\frac{\partial\omega_i}{\partial x_j} + \frac{\partial\omega_j}{\partial x_i}\right).$$

For a distinct body or region, and for small/incremental displacements, ω_i is unique only if rotation and strain are confined to discrete surfaces. Rigid body rotation is satisfied when $\varepsilon_{ij} = 0$ and $r_{ij} \neq 0$, and pure shear is achieved when $\varepsilon_{ij} \neq 0$ and $r_{ij} = 0$. In cases where $\varepsilon_{ij} \neq 0$, $r_{ij} \neq 0$, and both are continuous, vertical-axis rotations will vary systematically (e.g., along the strike of a curved orogen), so long as the entire curvature is due to rotation and strain.

For finite deformation, [D] = [T] [R] or [D] = [R] [U], where D is the total deformation, [T] and [U] are strain, [R] is rotation, and [T]≠[U] for the same [R]. Because multiplication is not commutative, the order in which rotation and strain are incorporated into the total deformation changes the results (Elliott, 1976b; Means, 1976; Ramsay, 1976).

The total amount of contractional deformation that takes place in a fold-and-thrust belt is used to: (1) compare contractions in different regions, (2) balance crustal masses in isostatic calculations, (3) generate palinspastic restorations of fold-and-thrust belts to their predeformed state, and (4) describe the geometry, kinematics, and dynamics of fold-and-thrust belt evolution. We define the total amount of shortening between two converging tectonic elements (i.e., plates, thrust sheets) as "tectonic shortening" to distinguish it from the amount of shortening contributed independently from translation, strain, and rotation. Since extension can take place in contractional regimes, which complicates shortening estimates, the term "contractional deformation" is defined as all those translations, rotations, and strains occurring in contractional regimes. The overall effect of tectonic shortening can be described by a finite rotation about an Euler pole on the surface of Earth.

Balanced cross sections have been used since the 1970s to measure amounts of contractional deformation in fold-and-thrust belts. For sections to fulfill the viability and admissibility criteria as defined by authors such as Dahlstrom (1969), Elliott (1972, 1983), Hossack (1979), Price (1981), and Woodward et al. (1989), the line of section must be drawn parallel to the transport direction and located at the apex of the curved map trace of a target thrust fault or orogen. In addition, cross sections through oblique zones or oblique ramps may be admissible, but they are not viable due to out-of-plane motions, if appropriate corrections are not considered (Cooper, 1983). The transport direction, internal strain, and rotations are all important factors that require consideration in the construction of cross sections and the way in which cross sections are used to quantify shortening.

For regional studies that rely on serial cross sections to understand an orogen in three dimensions, such sections either converge to a point in the hinterland (as in salients) or converge to a point in the foreland (as in recesses) (Woodward et al., 1986) (for examples, see Dixon, 1982; Kley and Monaldi, 1998). The resultant "fanning" of cross-section lines is also common when several local studies are compiled together, due to a generalized assumption that transport direction is perpendicular to strike. Price (1981), Cooper (1983), and Woodward et al. (1989) determined the errors in shortening estimates when cross sections are not drawn parallel to the transport direction. For example, an error of ≈15% occurs when a line of section is constructed 30° to tectonic transport, with principal errors resulting from overprojection of structures along-strike (Price, 1981; Woodward, 1989). Techniques by Cooper (1983) and DePaor (1988) help to resolve projection errors for map-scale structures in cross sections drawn oblique to the transport direction. Since transport directions can change temporally and spatially, such error corrections might involve several steps. Changes in the transport direction may be identifiable in the geologic record; for instance, Kwon and Mitra (2004) used structures associated with layer-parallel shortening and elastico-frictional deformation features to determine the early- and late-stage transport directions (respectively) in the Provo salient of the Sevier fold-and-thrust belt.

To produce as accurate a balanced section as possible, contributions from small-scale penetrative strains, as well as map-scale data (e.g., translations along faults and folding strains) need to be included to avoid errors that become cumulative across an orogen and can lead to inaccurate restored fold-and-thrust belt geometries (Mitra, 1994). The kinematic indicators associated with strains and the mechanisms that produce strains can also influence the kinematic admissibility of a section and ultimately the interpretation of an orogen's evolution (Geiser, 1988; Ferrill and Dunne, 1989; Mitra, 1994; Beaumont et al., 2000; Ismat and Mitra, 2005a). This is especially true when considering the range of deformational scales, such that it is important to define as precisely as possible the scale of the

features or phenomena being described. For example, the definition of "discrete" (for describing a fault) is a scale-dependent phenomenon, as exemplified by cataclastic flow, which is continuous at outcrop and larger scales but is discontinuous at smaller scales (e.g., Ismat and Mitra, 2005b).

Techniques for incorporating small-scale strains into balanced cross sections have been explained by various workers including: Woodward et al. (1986), Geiser (1988), Protzman and Mitra (1990), McNaught and Mitra, (1996), and Von Winterfeld and Oncken (1995). Though horizontal-axis rotations (due to folding) have been addressed by Mitra (1994) and Mukul and Mitra (1998), in this paper, we consider the impact of vertical-axis rotations on shortening estimates.

VERTICAL-AXIS ROTATIONS IN OROGENIC SYSTEMS

Diagnostic Measures

We refer to rotations of a volume about a vertical axis as a "coherent-body" rotation (a scenario in which the rotation tensor is continuous and reasonably uniform) because we recognize that deformation can also occur internal to the body. For this reason, we avoid the term "rigid-body" unless the only accommodation of a vertical-axis rotation is along the margins of the body such that internal strain $\varepsilon_{ij} = 0$. For rotating thrust sheets or tectonic plates, the distribution, magnitude, and direction of the rotations can be determined primarily through paleomagnetic analyses and subordinately through structural methods.

Paleomagnetic techniques can yield a quantifiable angle of rotation, and they allow for the identification of coherent-body vertical-axis rotations by comparing observed paleomagnetic declinations for a given time interval with expected paleomagnetic declinations from undeformed rocks magnetized during the same time interval. This assumes that the age of magnetization can be accurately determined, and that there is sufficient well-dated paleomagnetic data from the area of reference. In this sense, it is worth mentioning that paleomagnetic data must honor several reliability criteria to be considered robust (Van der Voo, 1990; Pueyo, 2010). A complete laboratory isolation of magnetic remanence components must be performed to avoid potentially large errors (Rodriguez et al., 2011). Evidences of internal deformation in the rock are enough to reject or to reevaluate paleomagnetic measurements (Lowrie et al., 1986; van der Pluijm, 1987; Kodama, 1988). Accurate restoration of paleomagnetic data to the appropriate reference frame also must be achieved, which is critical in complex portions of fold-and-thrust belts where noncoaxial axes of deformation have acted (e.g., conical and plunging folds, superimposed folding, forced folds, fold closures, oblique thrust ramps, etc.) (Stewart, 1995; Pueyo et al., 2003a, 2003b; Weil et al., 2000; Weil and Van der Voo, 2002).

Paleomagnetic data have been used to measure vertical-axis rotations in fold-and-thrust belts for nearly five decades (Norris and Black, 1961); some recent examples of investigations that have used paleomagnetic techniques for measuring vertical-axis rotations in orogenic systems include: (1) the Bolivian arc of the central Andes (e.g., Butler et al., 1995; Roperch et al., 2000; Arriagada et al., 2003, 2008); (2) the Pennsylvania salient in the central Appalachians (e.g., Schwartz and Van der Voo, 1984; Kent, 1988; Stamatakos and Hirt, 1994; Cioppa and Kodama, 2003); (3) the Southern Pyrenees (e.g., Dinarès et al., 1992; Pueyo, 2000; Sussman et al., 2003; Oliva-Urcia et al., 2008; Oliva et al., 2012; Mochales et al., 2012); (4) the Cantabrian-Asturian arc (e.g., Van der Voo et al., 1997; Weil et al., 2001; Weil, 2006); or (5) the Alps (Thöny et al., 2006; Pueyo et al., 2007).

Structural techniques typically document rotations by measuring components of the incremental strain field in different thrust sheets. For instance, Ferrill and Groshong (1993) used the temporal and spatial change of principal strain orientations from calcite twins to explain fold-and-thrust belt curvature in the Subalpine chain of France. In the Wyoming salient, Craddock et al. (1998), Apotria (1995), and Holl and Anastasio (1995) used similar data to document local thrust sheet rotations and variations in strain-axis orientations at oblique ramps. Using fault lineations and fold and axial trace geometries, respectively, Allerton (1998) and Oldow et al. (1990) determined relative thrust sheet rotations in the eastern Subbetic zone of southern Spain. Gray and Mitra (1993) and Kwon and Mitra (2004) conducted similar investigations in the Pennsylvania and Provo (Utah) salients, respectively. Hnat et al. (2008) and Pueyo-Anchuela et al. (2012) used, apart from paleomagnetism, the anisotropy of magnetic susceptibility (AMS) as an auxiliary tool to estimate vertical-axis rotation magnitudes. As such, structural techniques can provide constraints on the rotation history of a region by allowing for determination of the transport direction at different time intervals.

There are several regions in which structural and paleomagnetic techniques have both been used to understand the magnitude, direction, and distribution of rotations in fold-and-thrust belts. In some cases, the data from these different techniques are comparable, and in other cases, the techniques yield different results. For example, the predicted thrust rotations determined by Kollmeier et al. (2000) matched within error rotations determined from paleomagnetic analysis for the Cantabrian-Asturian arc (Weil et al., 2001). In the Subbetic zone, Allerton (1994) ascertained that thrust lineation rotations were constant relative to paleomagnetic rotations. Similarly, Oldow et al. (1990) and Channell et al. (1990), using fold geometries and paleomagnetism respectively, determined comparable rotation history for the Sicilian fold-and-thrust belt. On the other hand, in the Wyoming salient, the calcite twin data from Craddock et al. (1988) and paleomagnetic data from Grubbs and Van der Voo (1976) did not directly correspond. A similar discrepancy can be seen in the Swiss Jura, where rotational strain directions were not consistent with paleomagnetically measured vertical-axis rotations (Kempf et al., 1998; Hindle and Burkhard, 1999). Finally, paleomagnetic investigations in the Provo/Charleston-Nebo salient (Conder et al., 2003) are at odds with structural work by Kwon and Mitra (2004) in the same area. Such varied results reveal the complexity involved in incorporating all components of the total displacement field in developing reliable kinematic models (i.e., relationships among translation, strain, and rotation). The causes of these discrepancies are not fully understood, and they need to be defined for individual cases. Like Hindle and Burkhard (1999), who used varying data sets to successfully propose an integrated model for the Jura arc, Gray and Stamatakos (1997) also combined seemingly opposing data to develop a compelling integrated model for the Pennsylvania salient. Finally, consistent results from paleomagnetic, AMS, and calcite twinning allow rejection of any rotation in the interpretation of the kinematics of the Jones Valley thrust in the Appalachians (Hnat et al., 2008).

Since the rotational velocity and rotational ages (Pueyo et al., 2002; Mattei et al., 2004; Mochales et al., 2011) of thrust sheets are key variables, the effect of vertical-axis rotations must be removed at the proper time intervals during restoration to accurately determine the regional transport direction as well as the amount of rotational shortening. Integration of high-resolution paleomagnetic and structural data sets from strata of different ages and at the scale of individual thrust sheets is required to more accurately decipher the complex development of orogens that have undergone vertical-axis rotations.

Structures Accommodating Out-of-Plane Motion

Investigations from orogens worldwide show that a number of structures form to accommodate out-of-plane motion. For example, in the western Transverse Ranges of California, Onderdonk et al. (2005) demonstrated that

a zone of deformation, populated by folds, refolded folds, and reverse faults trending oblique and parallel to the two main bounding faults, accommodated the rotation between the bounding faults. Bayona et al. (2002) established the relationship between several transfer zones and rotations in the Southern Appalachians. Additionally, Berberian et al. (2000) suggested that a strike-slip fault connecting thrusts with opposite vergence took up vertical-axis rotations in the Sefidabeh area of the Sistan ranges in eastern Iran. Out-of-plane motion can also be accommodated by "thrust segmentation," such that an otherwise continuous thrust sheet is broken up by secondary structures, and/or variation in the along-strike nature of a fault or fault system, such as the Altyn Tagh in China (Rumelhart et al., 1999) or the southwestern Pyrenees in Spain (Pueyo et al., 1997). These investigations, as well as recent analogue modeling data (Soto et al., 2006), suggest that if the nature of along-strike shortening changes due to vertical-axis rotations, geologic structures that accommodate those changes will develop. Observations of accommodation structures raise several important questions:

(1) How do coherent bodies accommodate vertical-axis rotations?

(2) What features or group of features develop along the boundaries of such rotating bodies?

(3) How do these features change depending on the location of the rotation axis and timing relationships between translation and rotation?

To address these questions, we present several models for coherent-body rotations.

MODELS OF VERTICAL-AXIS ROTATIONS ASSOCIATED WITH THRUST SHEETS

Given a finite portion of a thrust surface, there are two scale-independent models that can be used to describe the effects of a rotational component on the total deformation field: (A) an internal pivot-point model (Figs. 2A and 2B) and (B) an external and/or termination pivot-point model (Figs. 2C and 2D), these models correspond to the near-field and

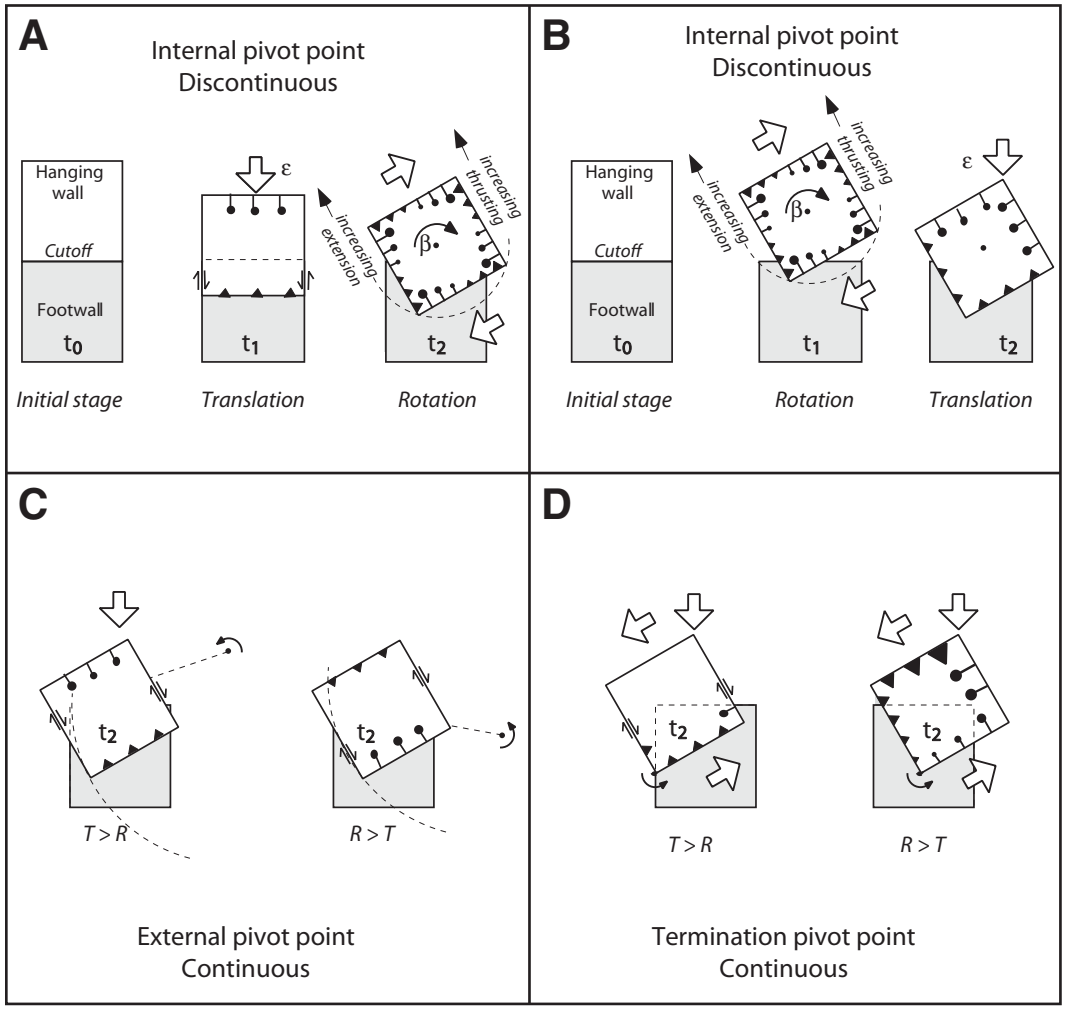

Figure 2. (A) Discontinuous deformation with internal pivot, part 1. t_0—Initial state. t_1—Translation results in strike-slip structures forming on the side edges of the sheet, with a thrust configuration on the leading edge of the sheet. t_2—During a counterclockwise rotation, this sheet would form thrust or normal fault structures on the edge of the sheet while reactivating the thrust on the leading edge of the sheet to a strike-slip boundary. The rotational motion would follow a small circle about a pivot. (B) Discontinuous deformation with internal pivot, part 2. t_0—Initial state. t_1—Rotation results in thrust or normal fault structures on the edge of the sheet. t_2—Translation during a second phase will be taken up by thrust motion at the corner and oblique slip along the edges of the sheet. Extension will occur in the rear of the sheet. (C) Continuous deformation with external pivot. (Left) Translation (*T*) occurs faster than rotation (*R*), giving rise to an oblique thrust relationship on the leading edge and strike-slip relationships on the sides. (Right) Rotation takes place faster than translation, yielding features such as normal faults on the leading edge and strike-slip faults on the sides. A comparison among part B, C, and D illustrates how the development of structures along the leading edge of a fault may allow for a first-order approximation of the general pivot location (i.e., internal or external) as well as an approximation of the relative timing of rates involved in deformation processes (rotation or translation). These models are predictive and need to be tested and verified with analyses of geological features in natural systems. See our example in the Wyoming salient. (D) Continuous deformation with termination pivot. A special case of deformation with an external pivot; the termination pivot follows Elliott's (1976a) "bow and arrow" rule, where a thrust tip marks the end of displacement. Geological examples of rotation with a termination pivot include Allerton (1994) and Pueyo (2000). (Left) Translation occurs at a faster rate than rotation and develops oblique slip on the sides with a thrust relationship along the leading edge of the body. This model probably represents the deformation processes acting at the crustal scale. (Right) Rotation outpaces translation, and extensional features develop along the frontal boundary of the body. This scenario is most likely restricted to the grain scale or the tectonic plate scale.

far-field concepts defined by Allerton (1998). Our analysis assumes that the pivot remains stationary throughout the motion of the body; if a rotation is caused by motion due to the presence of a preexisting structure (i.e., buttresses or lateral ramps), this simple approach is likely sufficient. On the other hand, if a rotation is the result of differential movement within a growing structure (e.g., thrust sheet or fold), then the pivot may move, and/or its position relative to the structure can change. As such, geologically meaningful pivots, such as a thrust termination/tip, represent only the pivot's final location such that a finite deformation is implied. If sufficient evidence is available to determine the incremental/continuous deformation and the stepwise location of the pivot, an approach similar to that proposed by Tikoff and Fossen (1995) can be applied.

In areas where thrust terminations are unavailable (e.g., eroded or covered), or to determine more precise pivot locations, high-resolution arrays of paleomagnetic vertical-axis rotation measurements need to be collected and merged with structural studies that yield transport directions. We propose that, rather than having a unique geological marker, suites of geologic structures can help identify whether or not a rotation occurred (e.g., Allerton, 1998; Rumelhart et al., 1999; Onderdonk et al., 2005), when the rotation took place with respect to translation, and the approximate location of the rotational pivot.

When a stationary pivot point is located inside a thrust sheet, the final geometry of the thrust sheet and its footwall is the same, but the geologic features that form during the deformation stages will be different. It is important to note that this scenario implies that all deformation is concentrated along the thrust sheet boundaries, rather than distributed within the sheet, probably a rare scenario to find in nature. In any case, timing effects are important. When translation is followed by a rotation such that [D] = [R] [U], part of frontal thrust boundary will be replaced by normal motion (Fig. 2A). The lateral lengthening of the contractional and extensional fronts will depend on the geometry of the hanging wall.

On the other hand, if a rotation occurs first such that [D] = [T] [R], the final feature to form will be a frontal thrust (Fig. 2B). Thus, if the pivot point is inside the block or thrust sheet (e.g., domino styles; McKenzie and Jackson, 1983; Ron et al., 1984; Garfunkel, 1989) and is in a fixed position throughout the active deformation, it may be possible to constrain timing relationships between translation and rotation by looking at geological features developed along the boundaries of the rotating object. A larger-scale demonstration of the concept is available in the North American plate (a plate-scale rotational block), which has a pivot within its body with respect to the Pacific plate/rotational block, such that the plate margins have similar boundaries to the example above. Likewise, with known timing relationships, the geological features might allow for the pivot location to be approximated.

When a thrust sheet undergoes translation and rotation with a pivot point located outside the sheet (Fig. 2C), the entire thrust sheet moves in the same direction, creating fewer space problems associated with bounding structures (Allerton, 1998). The farther a pivot point is from a thrust sheet, the more the effect from rotation is minimized such that displacement (deformation) trajectories can be simplified as a translation. In this case, the geologic features that form may include normal faults that are later reactivated as thrust faults (rotation followed by translation; Fig. 2C, left), or thrust faults reactivated as normal faults (translation followed by rotation; Fig. 2C, right). Likewise, a scenario with simultaneous rotation and translation will produce similar features depending on the deformation rates of the various processes (Fig. 2C).

A pivot point that exists at the end of a fault can be called a "termination pivot" (Fig. 2D); we propose a termination pivot model to be the most applicable for developing thrust structures (and listric normal faults). A useful concept that explains our rationale is Elliott's "bow and arrow rule" (1976a), in which the normal bisector of a straight line, drawn between the terminations of a curved thrust, yields the maximum displacement of that thrust with a decrease of displacement toward the tips, so long as the transport direction is parallel to the bisector. Self-similar "bow and arrow" thrust growth, in which thrust length and displacement along the normal bisector increase proportionately, requires nonzero strain and rotation tensors, where $\varepsilon_{ij} \neq 0$ and $r_{ij} \neq 0$. It is at the tips of these thrusts, however, where strain and rotation are both zero, that pivots are located at the terminations on either end of the thrust. Allerton (1994) documented an along-strike increase in shortening from a pivot located on the end of a "bow and arrow" and identified the pivot point of a rotating structure at its termination by measuring folding strain and paleomagnetically determining vertical-axis rotations in the Subbetics of southern Spain. Similar results are found in the south Pyrenean sole thrust in the Central Pyrenees (Millán et al., 1995, 2000; Pueyo et al., 1999; Oliva-Urcia et al., 2010), where the westernmost termination of the External Sierras thrust front ends in a detachment anticline followed by a more steeply plunging fold (the San Marzal fold-closure).

For a comprehensive analysis of the effect that a termination pivot point has on shortening, imagine a surface element deformed in a discontinuous fashion (Fig. 3A), first by translation (ε), with the transport direction perpendicular to the hanging wall thrust trace, followed by a coherent body rotation about a vertical axis (β). For equal amounts of rotation and translation, the sequential order of the operative mechanism will play a definitive role in the final location of the initial element and, thus, is noncommutative (Fig. 3A). Also, note the centripetal migration of the rotation pivot point. Regardless of the first motion, the location of the final pivot point will be controlled by the sequence and magnitude of both deformational processes. In any case, a circular path will be able to relate the initial (nondeformed) and the final (deformed) stages.

Given a continuously developing thrust system, we illustrate several merged increments of translation and coherent body rotations (Fig. 3B). In the general case, an ellipse best relates the initial to the final deformation processes, including noncommutative translations and rotations. However, except for extreme and complex translation/rotation ratios that need to be individually calculated, the eccentricity of the ellipse will be very low, and so a circular path is employed in our model for mathematical simplicity. The elliptical trajectory defining the movement of a hanging-wall point depends on the translation and rotation magnitudes and their temporal relationship. In extreme translation/rotation ratios, this mathematical function may be very complex and would have to be calculated for each individual case. In most other cases, however, the eccentricity of the ellipse will be very low and can be easily approached by the circular paths represented in our model.

A map-view model displaying the trigonometric relations between the footwall and hanging-wall cutoffs in a rotational setting was proposed by Pueyo (2000) and Pueyo et al. (2004). This model (Fig. 4A) relates the true shortening (S and S′, assuming a stationary pivot) with the measured shortening from a balanced cross section (Sm), if the rotation (β) has not been considered.

Imagine a cross section drawn perpendicular to the footwall cutoff (Fig. 4A), parallel to the transport direction, and located at a fixed distance from the pivot point (for cross sections oblique to the transport direction, an extra correction is needed; e.g., Cooper, 1983; DePaor, 1988; Pueyo et al., 2004). When the cross section is restored, Sm represents the measured cross-sectional shortening, but due to out-of-plane motion, this value is in error and needs to be corrected. Given a known rotation angle (β) (e.g., determined by paleomagnetic analysis), the true shortening (S) along the selected line can be determined. By virtue of the sine law, the shortening along the chord (S′) will be:

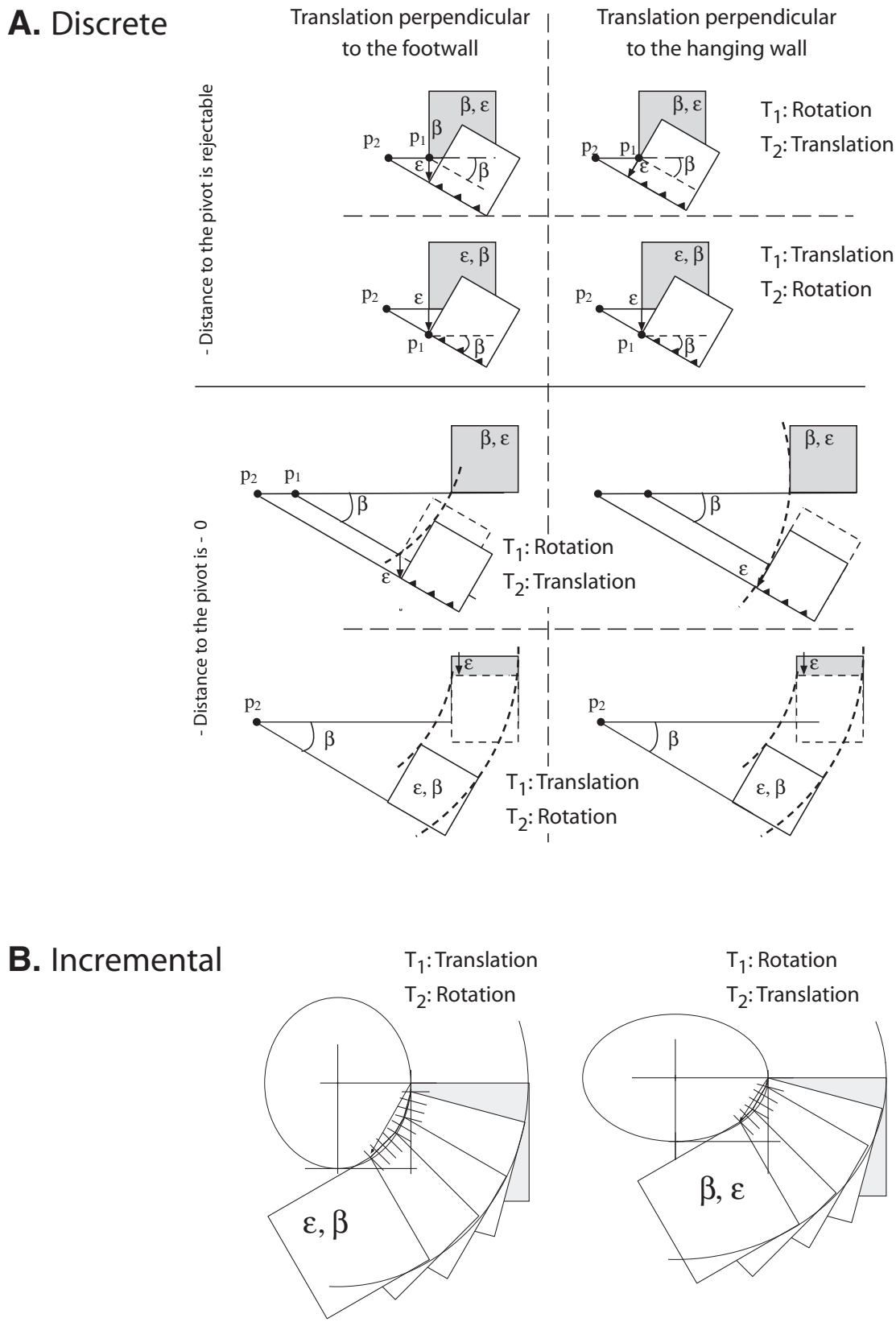

Figure 3. Trigonometric models showing map-view spatial relations among translation (ε), rotation (β), the transport direction, and the pivot in a deformed surface element (white). Undeformed stage (gray) has been drawn to allow for comparison. (A) Discontinuous sequences produce different final stages (noncommutative) depending upon the aforementioned variables. (B) Continuous process (mixed infinitesimal rotations and translation).

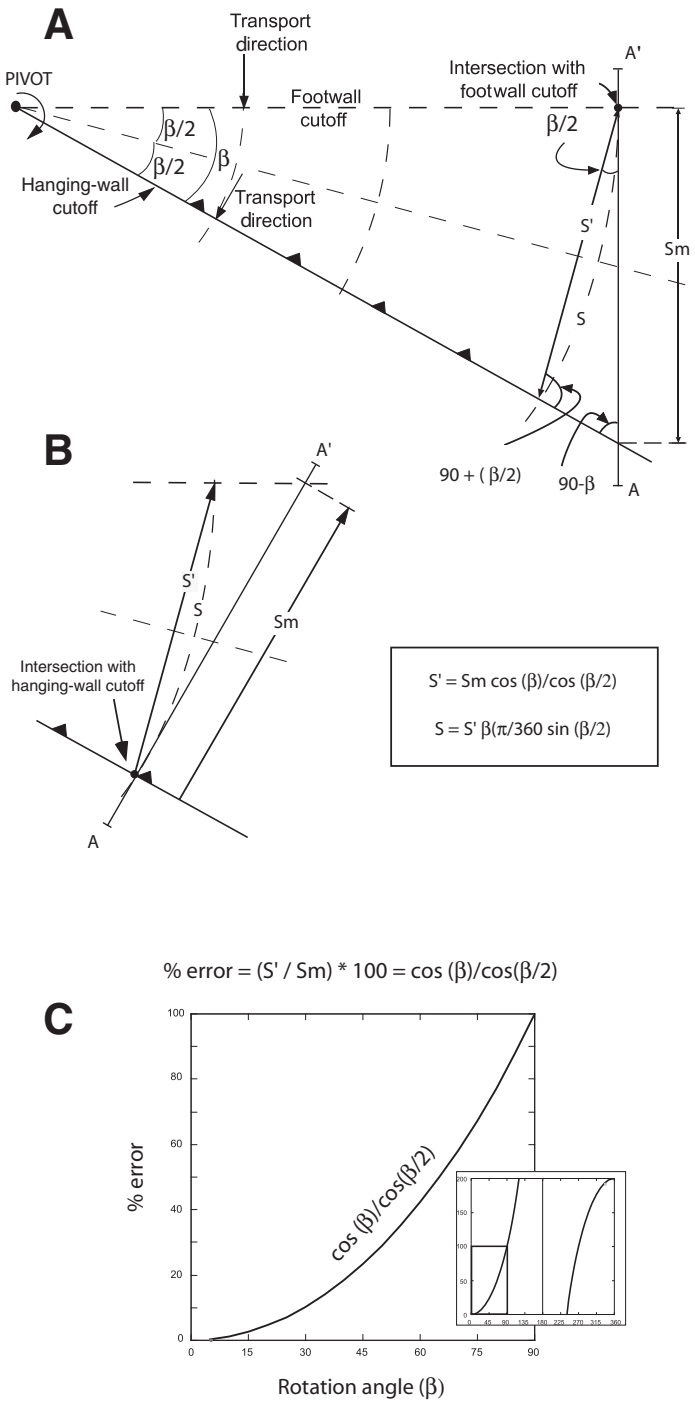

Figure 4. (A) Trigonometric relationships among hanging-wall and footwall cutoffs, the rotation angle (β), and three possible calculations of shortening; Sm—measured shortening without considering rotation, S′—the chord of the curved trajectory, S—the "true" curved path. The transport direction is perpendicular to the hanging-wall cutoff (Pueyo et al., 2004). The cross-section line A–A′ is perpendicular to the footwall cutoff. (B) Same model with cross-section line A–A′ perpendicular to hanging-wall cutoff. (C) Nomogram displaying the graphic relation between the rotation (β) and the expected error, if the restoration is done without taking into account the rotation. The error function has been calculated using the shortening function by Pueyo et al. (2004). The most plausible rotation angles in geological situations have been represented, with the whole function plotted in the inset.

$$S' = Sm\sin(90-\beta)/\sin(90+\beta/2) = Sm\cos(\beta)/\cos(\beta/2), \quad (1)$$

with the true minimum shortening (S) along the arc:

$$S = S'\beta\pi/360\sin(\beta/2) = Sm\beta\pi/180\tan(\beta). \quad (2)$$

Comparing the measured shortening (Sm) with the shortening along the chord (S′), the error is:

$$\%Error = \left[1-(S'/Sm)\right]\times 100 = \left\{1-\left[\cos(\beta)/\cos(\beta/2)\right]\right\}\times 100. \quad (3)$$

Similarly, along the arc, the error is:

$$\%Error = \left[1-(S/Sm)\right]\times 100 = \left\{1-\left[\beta\pi/180\tan(\beta)\right]\right\}\times 100. \quad (4)$$

A graph of this trigonometric function (Fig. 4C) calculates the percent error in shortening given the above conditions. For example, vertical-axis rotations of 80° will produce an apparent shortening almost double that of the true shortening, if the cross section is drawn in a straight line perpendicular to the thrust trace. For β = 50°, the measured shortening will contain a 30% error. Rotations below 30° generate errors <10%. These calculations will need an additional correction, if the cross section is not drawn parallel to the transport direction (Cooper, 1983; DePaor, 1988; Pueyo et al., 2004).

APPLICATION TO THE WYOMING SALIENT

The Sevier fold-and-thrust belt of Idaho, Utah, and Wyoming (Armstrong, 1968) defines the eastern margin of the Cordilleran orogen in western North America. Proterozoic, Paleozoic, and Mesozoic sedimentary rocks in this area underwent shortening and translation during the late Jurassic to early Eocene Sevier orogeny (Burchfiel and Davis, 1975), with successive thrusts generally forming eastward in time with transport in that direction (e.g., Armstrong and Oriel, 1965; Royse et al., 1975; Jordan, 1981) and continued reactivation in the back of the orogen (DeCelles and Mitra, 1995). The Sevier fold-and-thrust belt is divided into a number of salients (Smith and Bruhn, 1984; Lawton et al., 1994), each convex to the foreland. The Wyoming salient, located in western Wyoming, southeastern Idaho, and northeastern Utah, is bounded to the north by the Gros Ventre and Wind River Ranges, to the south by the Uinta Arch, and to the east by the Hoback and Green River basins. From the hinterland to the foreland, the major thrusts in the northern Wyoming salient are: the Paris, Meade, Absaroka, Darby, and Prospect thrusts (Fig. 5).

Wyoming Salient: Geologic Features

The curved nature of the Wyoming salient has been well-studied by a number of workers and is generally considered to be the result of buttressing effects from the Teton–Gros Ventre and other basement uplifts to the east (Crosby, 1969; Grubbs and Van der Voo, 1976; Beutner, 1977; Blackstone, 1977; Dorr et al., 1977; Wiltschko and Dorr, 1983; Hunter, 1988; Weil and Yonkee, 2009; Yonkee and Weil, 2010; Weil et al., 2010). However, Woodward et al. (1986) and Royse (1993) suggested that stratigraphic controls play a larger role than buttressing in determining regional along-strike changes. Dixon (1982) used industry seismic data to construct ~50 cross sections, providing insight into the along-strike variations of structures within the salient (Fig. 5A). In particular, the Prospect thrust shows significant variation in the amount of displacement along strike (Dixon, 1982). The differential transport implied by the bulk shear angles (up to 48°) in parts of the Prospect thrust predicts the presence of oblique

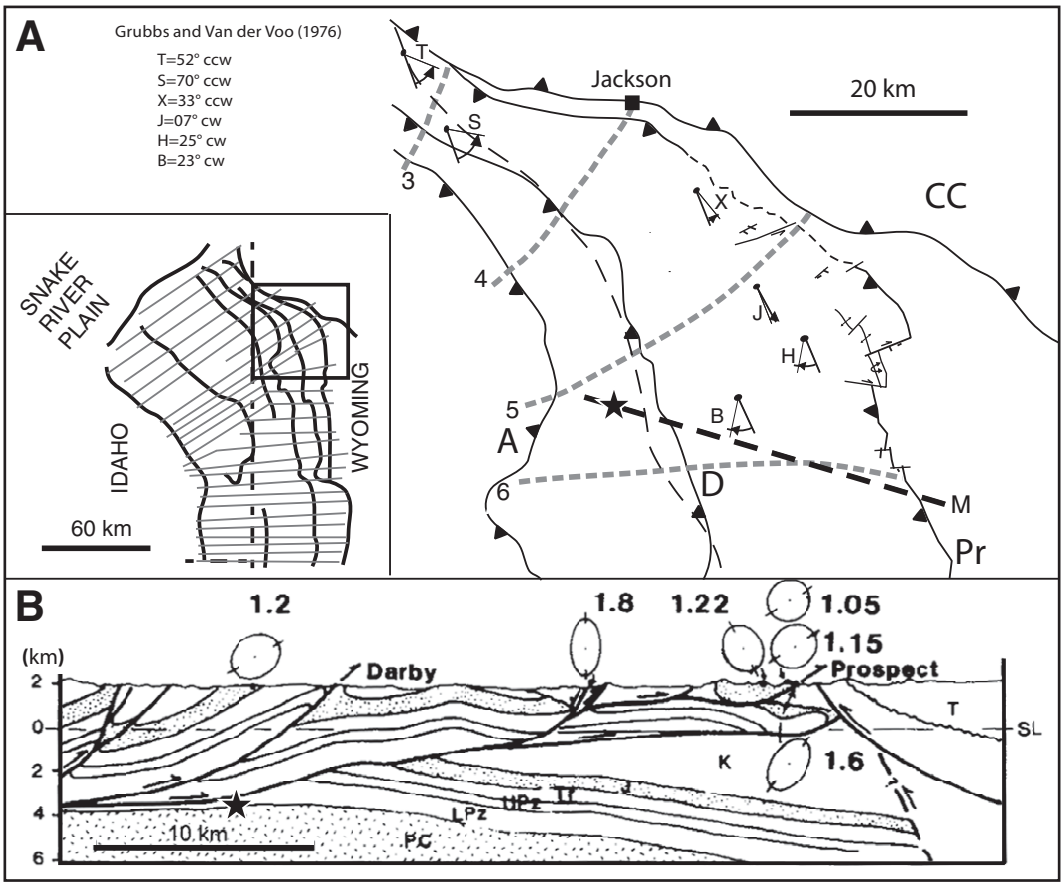

Figure 5. The Wyoming salient. (A) Composite map showing data from Craddock et al. (1988), numbered deformation paths in gray dashes; Dorr et al. (1977) and Hunter (1988), details of Prospect thrust front geometry; and Grubbs and Van der Voo (1976), vertical-axis rotation based on paleomagnetic data. For the paleomagnetic data, the angle between the fixed direction reference line (thick) and the observed direction line (thin) represents the magnitude and direction of rotation of the observed direction line with respect to the fixed reference line. Mitra's (1994) line of section is shown with double dashes, with a filled star representing the trailing branch line of the Lower Paleozoic for the Prospect thrust. The black dashed line depicts the footwall cutoff of the Prospect thrust. Inset: Regional map from Dixon (1982) showing the extensive number of cross sections drawn and traces of major thrusts. (B) Mitra's (1994) cross section including strain ellipses used in his shortening calculation.

ramps and tear faults along the thrust trace (Wilkerson, 1992). Similarly, Apotria (1995) modeled particle paths for oblique ramps in this region and found that out-of-plane strains are taken up by footwall geometries and varying amounts of thrust displacement, which manifest themselves as accommodation structures. In fact, the Prospect thrust is highly segmented (Fig. 5A) by tear, strike-slip, and normal faults oriented perpendicular to the thrust front (Dorr et al., 1977; Blackstone, 1977; Hunter, 1987). The geologic characteristics reported in these investigations suggest that vertical-axis rotations occurred in the Wyoming salient.

Diagnostic Measures of Vertical-Axis Rotations in the Wyoming Salient

Variations in the transport direction and vertical-axis rotations within the Wyoming salient have been documented by paleomagnetic and structural studies. Several workers, including Craddock et al. (1988), Mitra (1994), Apotria, (1995), and Yonkee and Weil (2010), documented out-of-plane strains from small-scale structures. For example, Craddock et al. (1988) used calcite twin strains to suggest curved deformation paths for material within the Wyoming salient. The strain trajectories due to layer-parallel shortening determined by Craddock et al. (1988) vary from counterclockwise in the northern part of the salient to clockwise in the southern part of the salient. Data such as this allow us to reconstruct the early transport direction of material within the Wyoming salient.

In addition, vertical-axis rotations from paleomagnetic data were measured in the Wyoming salient by Grubbs and Van der Voo (1976), Eldredge and Van der Voo (1988), and Weil et al. (2010). McWhinnie et al. (1990) suggested that the vertical-axis rotations of the Prospect thrust sheet likely occurred contemporaneously with thrust motion. Based on Sussman et al. (2003), Weil and Sussman (2004), and Weil et al. (2010), this portion of the Wyoming salient can be considered a progressive arc, such that the pivot location may not have been fixed through time during deformation. The structures that developed along the thrust front reflect the expected accommodation styles based on an external pivot point model (Fig. 2C).

Several workers (e.g., Royse et al., 1975; Blackstone, 1977; Dorr et al., 1977; Dixon, 1982; Woodward et al., 1986; Craddock, 1992; Mitra, 1994; Yonkee and Weil, 2010) have calculated shortening across the northern Wyoming salient (or portions thereof). While most of these authors based their estimates on translational shortening and folding strain, Craddock (1992), Mitra (1994), and Yonkee and Weil (2010) also included internal strains in their estimates.

Impact of Vertical-Axis Rotation on Shortening Estimates in the Wyoming Salient

Paleomagnetic analyses (Grubbs and Van der Voo, 1976; Weil et al., 2010) have shown that the Prospect thrust sheet has undergone extensive and systematic rotation (Fig. 5A); thus, we focus our example on the Prospect sheet to estimate the amount of shortening error due to neglecting the contribution of coherent body rotation. To incorporate the rotational component into total shortening estimates, we first examine the transport direction.

Curved strain trajectories from calcite twinning, cleavage, and other structures developed during layer-parallel shortening (Craddock et al., 1988; Yonkee and Weil, 2009), and paleomagnetic data (Grubbs and Van

der Voo, 1976; Weil et al., 2010) have been used to constrain the early transport direction of the Prospect thrust sheet. Since layer-parallel shortening develops early in the deformational history of the thrust sheet, any later coherent body rotations would have passively rotated the preexisting strain trajectories, and their implied transport direction. For our analysis in the Wyoming salient, we have chosen a reference point (Fig. 5A, star) that represents the footwall cutoff of the Prospect thrust in Mitra's (1994) cross section (Fig. 5B). We used the divergent calcite twin paths (Craddock et al., 1988) to interpolate the transport direction at the point indicated (Fig. 6A) in the footwall cutoff in the Prospect thrust. Since the transport direction recorded by the calcite twins at that point has been passively rotated by vertical-axis rotations (Grubbs and Van der Voo, 1976; Weil et al., 2010), the transport direction must be rotated to obtain the original direction of thrust motion. We have rotated this layer-parallel shortening transport direction by 33° in a counterclockwise direction to reflect the 33° clockwise rotation about a vertical axis as determined by Grubbs and Van der Voo (1976); likewise, vertical-axis rotation results from Weil et al. (2010) range from 20° to 40°.

The Prospect thrust rotation pivot (Fig. 6B, "pivot") had to satisfy the following requisites: (1) A circle centered on this pivot must be tangent

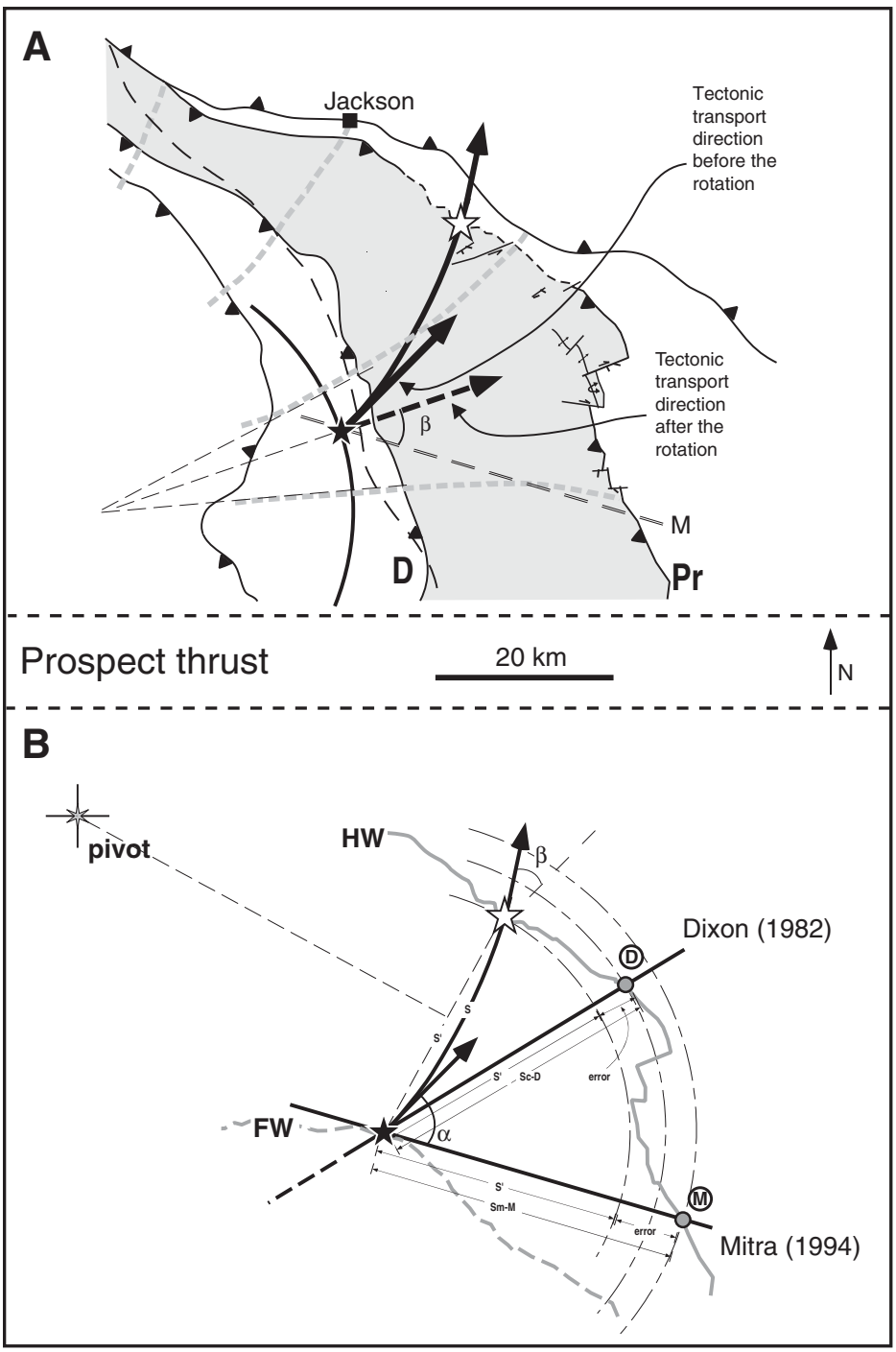

Figure 6. (A) Estimation of the transport direction. The filled star is the footwall cutoff in the Prospect thrust sheet corresponding to Mitra's (1994) cross section. The open star is the hanging-wall cutoff. The gray dashed lines represent the particle paths from Craddock et al. (1988). These have been rotated 33° counterclockwise to account for the later 33° clockwise rotation recorded by Grubbs and Van der Voo (1976), and angles are labeled on the map. (B) Map-view model, showing a close-up of the area with the lines of section from Dixon (1982) and Mitra (1994) that we used to calculate shortening errors due to vertical-axis rotations. The thin black dashed path is the curved line along which a cross section would incorporate the rotation. We estimate the error in previous sections (Mitra, 1994; Dixon, 1982) by comparing them with the chord length of this curved line. Refer to text for details. FW—footwall; HW—hanging wall.

to the transport direction at the Prospect footwall cutoff point. This path represents the actual trajectory followed by material in the hanging wall of the Prospect thrust. Importantly, in any orogenic system where vertical-axis rotations have been documented, all cross sections should be drawn along curved lines reflecting the real movement of the particles. (2) The intersection of the circle in the hanging-wall cutoff must be tangential to the rotated transport direction (Fig. 6). From the thrust "pivot," the measured angle between the footwall and hanging-wall cutoffs (Fig. 6B) must be equal to the paleomagnetic rotation. If other portions of the Prospect sheet, or areas of the Wyoming salient, are considered, different pivot locations will be found.

A trigonometric map-view model has been built for the Prospect thrust sheet of the Wyoming salient (Fig. 6B). The first observation is that the real tectonic transport trajectory (see previous explanation) is located far from the line of section drawn by Dixon (1982, labeled D). Through application of Equation 2, we find an overestimation of the shortening along the Prospect thrust of ~14%. It is important to mention that such errors are cumulative and depend on the misorientation of the transport direction, as well as from having ignored vertical-axis rotation (not incorporating the effects of penetrative strain [Mitra, 1994] may add more error). For the portion of the Prospect thrust sheet investigated, the error introduced into these sections from neglecting the 33° clockwise vertical-axis rotation (Grubbs and Van der Voo, 1976) is ~11%. The remaining error (~3%) is due to the oblique orientation of the cross section with respect to the real transport direction.

Layer-parallel shortening data from transects farther to the south (Mitra, 1994) indicate uniform transport direction for those southerly transects (Figs. 5 and 6A). Thus, in this more southern area, Dixon's other cross sections would yield a better approximation of shortening. Given this distinction, a change in the type of deformation could be indicated such that in the more curved portion of a thrust sheet, particle paths are radial, whereas in the straighter portions, particle paths are straight and parallel. Therefore, in the curved portions, restorations would result in excess volume at the point at which the radial sections converge.

CONCLUSIONS

Tectonic shortening is the total amount of deformation between two converging bodies and can be completely described by the displacement field, which consists of three components of deformation: translation, rotation, and strain. Neglecting the contribution of vertical-axis rotations may lead to inaccurate estimations of tectonic shortening, causing misunderstandings as to the kinematic and mechanical development of orogenic systems. This investigation indicates that shortening estimates that take rotations into account will differ from those estimates that do not incorporate rotations. We have calculated errors for previous estimations of the tectonic shortening for the Prospect thrust sheet of the northern portion of the Wyoming salient. This was accomplished by combining structural analyses, which have independently calculated translation and strain shortening, with a trigonometric function that incorporates the contribution from rotational shortening. The rotational contribution toward tectonic shortening was determined by analyzing the paleomagnetic evidence for regional (coherent and/or rigid) vertical-axis rotations in conjunction with field and microstructural evidence of such rotations. The relative timing of these deformation processes plays a role in the development of various geological features. We propose that suites of geologic features (thrust segmentation, etc.) suggest that vertical-axis rotations have taken place, can aid in determining the relative timing of rotation with translation, and can provide constraints as to the location of the rotation axis, or pivot point. Collection of high-resolution data sets of vertical-axis rotations and further integration of paleomagnetic analyses and structural studies in other orogens are needed in order to more accurately measure tectonic shortening.

ACKNOWLEDGMENTS

We thank Ruth Soto Marin and an anonymous reviewer for their suggestions and improvements on this paper. We also thank David Ferrill and Robert Butler for their comments on an earlier version of this manuscript. Support for this work was provided by the American Chemical Society to Chase and Sussman and from the Pmag3Drest (CGL2009-14214 MICINN) and 3DR3 (PI165/09 Aragonian government) to E.L. Pueyo. Finally, we are forever grateful for and remember Martin Burkhard.

REFERENCES CITED

Allerton, S., 1994, Vertical-axis rotation associated with folding and thrusting: An example from the eastern Subbetic zone of southern Spain: Geology, v. 22, no. 11, p. 1039–1042, doi:10.1130/0091-7613(1994)022<1039:VARAWF>2.3.CO;2.

Allerton, S., 1998, Geometry and kinematics of vertical-axis rotations in fold and thrust belts: Tectonophysics, v. 299, p. 15–30, doi:10.1016/S0040-1951(98)00196-6.

Apotria, T.G., 1995, Thrust sheet rotation and out-of-plane strains associated with oblique ramps: An example from the Wyoming salient: Journal of Structural Geology, v. 17, no. 5, p. 647–662, doi:10.1016/0191-8141(94)00087-G.

Armstrong, F.C., and Oriel, S.S., 1965, Tectonic development of the Idaho-Wyoming thrust belt: American Association of Petroleum Geologists Bulletin, v. 49, p. 1847–1866.

Armstrong, R.L., 1968, Sevier orogenic belt in Nevada and Utah: Geological Society of America Bulletin, v. 79, p. 429–458, doi:10.1130/0016-7606(1968)79[429:SOBINA]2.0.CO;2.

Arriagada, C., Roperch, P., Mpodozis, C., Dupont-Nivet, G., Cobbold, P.R., and Cauvin, A., 2003, Paleogene clockwise tectonic rotations in the fore-arc of central Andes, Antofagasta region, northern Chile: Journal of Geophysical Research, v. 108, 2032, doi:10.1029/2001JB001598.

Arriagada, C., Roperch, P., Mpodozis, C., and Cobbold, P.R., 2008, Paleogene building of the Bolivian orocline: Tectonic restoration of the central Andes in 2-D map view: Tectonics, 27, TC6014, 14 p.

Bayona, G., Thomas, W.A., and Van der Voo, R., 2002, Kinematics of thrust sheets within transverse zones: A structural and paleomagnetic investigation in the Appalachian thrust belt of Georgia and Alabama: Journal of Structural Geology, v. 25, p. 1193–1212, doi:10.1016/S0191-8141(02)00162-1.

Beaumont, C., Muñoz, J.A., Hamilton, J., and Fullsack, P., 2000, Factors controlling the Alpine evolution of the central Pyrenees inferred from a comparison of observations and geodynamical models: Journal of Geophysical Research, ser. B, Solid Earth and Planets, v. 105, no. 4, p. 8121–8145.

Berberian, M., Jackson, J.A., Qorashi, M., Talebian, M., Khatib, M., and Priestley, K., 2000, The 1994 Sefidabeh earthquakes in eastern Iran: Blind thrusting and bedding-plane slip on a growing anticline, and active tectonics of the Sistan suture zone: Geophysical Journal International, v. 142, p. 283–299, doi:10.1046/j.1365-246x.2000.00158.x.

Beutner, E.C., 1977, Causes and consequences of curvature in the Sevier orogenic belt, Utah to Montana, *in* Helsey, E.L., Lawson, D.E., Norwal, E.R., Wach, P.H., and Hale, L.E., eds., Rocky Mountain Thrust Belt, Geology and Resources: Wyoming Geological Association Guidebook, v. 29, p. 353–365.

Blackstone, D., 1977, The Overthrust belt salient of the Cordilleran fold belt—Western Wyoming, southeastern Idaho, northeastern Utah, *in* Helsey, E.L., Lawson, D.E., Norwal, E.R., Wach, P.H., and Hale, L.E., eds., Rocky Mountain Thrust Belt, Geology and Resources: Wyoming Geological Association Guidebook, v. 29, p. 367–384.

Burchfiel, B.C., and Davis, G.A., 1975, Nature and control of Cordilleran orogenesis, western United States—Extensions of an earlier synthesis: American Journal of Science, v. 275A, p. 363–396.

Butler, R.F., Richards, D.R., Sempere, T., and Marshall, L.G., 1995, Paleomagnetic determinations of vertical-axis tectonic rotations from Late Cretaceous and Paleocene strata of Bolivia: Geology, v. 23, p. 799–802, doi:10.1130/0091-7613(1995)023<0799:PDOVAT>2.3.CO;2.

Channell, J.E.T., Oldow, J.S., and Catalano, R., 1990, Paleomagnetically determined rotations in the western Sicilian fold and thrust belt: Tectonics, v. 9, p. 641–660, doi:10.1029/TC009i004p00641.

Cioppa, M.T., and Kodama, K.P., 2003, Evaluation of paleomagnetic and finite strain relationships due to the Alleghanian orogeny in the Mississippian Mauch Chunk Formation, Pennsylvania: Journal of Geophysical Research, ser. B, Solid Earth and Planets, v. 108, no. 2, 16 p.

Cobbold, P.R., 1979, Removal of finite deformation using strain trajectories: Journal of Structural Geology, v. 1, no. 1, p. 67–72, doi:10.1016/0191-8141(79)90022-1.

Conder, J., Butler, R.F., DeCelles, P.G., and Constenius, K.N., 2003, Paleomagnetic determination of vertical-axis rotations in the Charleston-Nebo salient: Utah Geology, v. 31, p. 1113–1116, doi:10.1130/G19893.1.

Cooper, M.A., 1983, The calculation of bulk strain in oblique and inclined balanced sections: Journal of Structural Geology, v. 5, no. 2, p. 161–165, doi:10.1016/0191-8141(83)90041-X.

Craddock, J.P., 1992, Transpression during tectonic evolution of the Idaho-Wyoming fold-and-thrust belt, *in* Link, P.K., Kuntz, M.A., and Platt, L.B., eds., Regional Geology of

Eastern Idaho and Western Wyoming: Geological Society of America Memoir 179, p. 125–139.
Craddock, J.P., Kopania, A.A., and Wiltschko, D.V., 1988, Interaction between the northern Idaho-Wyoming thrust belt and bounding basement blocks, central western Wyoming, *in* Schmidt, C.J., and Perry, W.J., Jr., eds., Interaction of the Rocky Mountain Foreland and the Cordilleran Thrust Belt: Geological Society of America Memoir 171, p. 333–351.
Crosby, G.W., 1969, Radial movements in the western Wyoming salient of the Cordilleran Overthrust belt: Geological Society of America Bulletin, v. 80, p. 1061–1077, doi:10.1130/0016-7606(1969)80[1061:RMITWW]2.0.CO;2.
Dahlstrom, C.D.A., 1969, Balanced cross sections: Canadian Journal of Earth Sciences, v. 6, p. 743–757, doi:10.1139/e69-069.
DeCelles, P.G. and Mitra, P.G., 1995, History of the Sevier orogenic wedge in terms of critical taper models, northeast Utah and southwest Wyoming: Geological Society of America Bulletin, v. 107, p 454–462.
DePaor, D.G., 1988, Balanced section in thrust belts: American Association of Petroleum Geologists Bulletin, v. 72, p. 73–82.
Dinarès, J., McClelland, E., and Santanach, P., 1992, Contrasting rotations within thrust sheets and kinematics of thrust tectonics as derived from palaeomagnetic data: An example from the Southern Pyrenees, *in* McClay, K.R., ed., Thrust Tectonics: London, Chapman and Hall, p. 265–275.
Dixon, J.S., 1982, Regional structural synthesis, Wyoming salient of the Western Overthrust belt: American Association of Petroleum Geologists Bulletin, v. 10, p. 1560–1580.
Dorr, J.A., Jr., Spearing, D.R., and Steidtman, J.R., 1977, Deformation and Deposition between a Foreland Uplift and an Impinging Thrust Belt, Hoback Basin, Wyoming: Geological Society of America Special Paper 177, 82 p.
Dunbar, J.A., and Cook, R.W., 2003, Palinspastic reconstruction of structure maps: An automated finite element approach with heterogeneous strain: Journal of Structural Geology, v. 25, p. 1021–1036, doi:10.1016/S0191-8141(02)00154-2.
Eldredge, S., and Van der Voo, R., 1988, Paleomagnetic study of thrust sheet rotations in the Helena and Wyoming salients of the northern Rocky Mountains, *in* Schmidt, C.J., and Perry, W.J., Jr., eds., Interaction of the Rocky Mountain Foreland and the Cordilleran Thrust Belt: Geological Society of America Memoir 171, p. 319–332.
Elliott, D., 1972, Deformation paths in structural geology: Geological Society of America Bulletin, v. 83, p. 2621–2635, doi:10.1130/0016-7606(1972)83[2621:DPISG]2.0.CO;2.
Elliott, D., 1976a, The motion of thrust sheets: Journal of Geophysical Research, v. 81, p. 949–963, doi:10.1029/JB081i005p00949.
Elliott, D., 1976b, The energy balance and deformation mechanisms of thrust sheets: Philosophical Transactions of the Royal Society of London, v. 283, p. 289–312, doi:10.1098/rsta.1976.0086.
Elliott, D., 1983, The construction of balanced cross sections: Journal of Structural Geology, v. 5, p. 101, doi:10.1016/0191-8141(83)90035-4.
Erickson, S.G., Hardy, S., and Suppe, J., 2000, Sequential restoration and unstraining of structural cross sections: Applications to extensional terranes: American Association of Petroleum Geologists Bulletin, v. 84, no. 2, p. 234–249.
Ferrill, D.A., and Dunne, W.M., 1989, Cover deformation above a blind duplex: An example from West Virginia: Journal of Structural Geology, v. 11, p. 421–431, doi:10.1016/0191-8141(89)90019-9.
Ferrill, D.A., and Groshong, R.H., 1993, Kinematic model for the curvature of the northern Subalpine Chain, France: Journal of Structural Geology, v. 15, no. 3–5, p. 523–541.
Garfunkel, Z., 1989, Regional deformation by block translation and rotation, *in* Kissel, C., and Laj, C., eds., Paleomagnetic Rotations and Continental Deformation: Nato ASI Series C, Boston, Kluwer Academic Publishers, v. 254, p. 181–208.
Geiser, P.A., 1988, The role of kinematics in the construction and analysis of geologic cross sections in deformed terranes, *in* Mitra, G., and Wojtal, S., eds., Geometries and Mechanics of Thrusting with Special Reference to the Appalachians: Geological Society of America Special Paper 222, p. 47–76.
Gray, M.B., and Mitra, G., 1993, Migration of deformation fronts during progressive deformation: Evidence from detailed structural studies in the Pennsylvania Anthracite region, USA: Journal of Structural Geology, v. 15, p. 435–449, doi:10.1016/0191-8141(93)90139-2.
Gray, M.B., and Stamatakos, J., 1997, New model for evolution of fold and thrust belt curvature based on integrated structural and paleomagnetic results from the Pennsylvania salient: Geology, v. 25, no. 12, p. 1067–1070, doi:10.1130/0091-7613(1997)025<1067:NMFEOF>2.3.CO;2.
Groshong, R.H., 1972, Strain calculated from twinning in calcite: Geological Society of America Bulletin, v. 83, p. 2025–2038, doi:10.1130/0016-7606(1972)83[2025:SCFTIC]2.0.CO;2.
Grubbs, K.L., and Van der Voo, R., 1976, Structural deformation of the Idaho–Wyoming Overthrust belt (U.S.A.), as determined by Triassic paleomagnetism: Tectonophysics, v. 33, p. 321–336, doi:10.1016/0040-1951(76)90151-7.
Guzofski, C.A., Mueller, J.P., Shaw, J.H., Muron, P., Medwedeff, D.A., Bilotti, F., and Rivero, C., 2009, Insights into the mechanisms of fault-related folding provided by volumetric structural restorations using spatially varying mechanical constraints: American Association of Petroleum Geologists Bulletin, v. 93, no. 4, p. 479–502, doi:10.1306/11250807130.
Hindle, D., and Burkhard, M., 1999, Strain, displacement and rotation associated with the formation of curvature in fold belts: An example from the Jura arc: Journal of Structural Geology, v. 21, p. 1089–1101, doi:10.1016/S0191-8141(99)00021-8.
Hnat, J.S., van der Pluijm, B.A., Van der Voo, R., and Thomas, W.A., 2008, Differential displacement and rotation in thrust fronts: A magnetic, calcite twinning and palinspastic study of the Jones Valley thrust, Alabama, U.S. Appalachians: Journal of Structural Geology, v. 30, no. 6, p. 725–738, doi:10.1016/j.jsg.2008.01.012.
Holl, J.E., and Anastasio, D.J., 1995, Kinematics around a large-scale oblique ramps, Southern Pyrenees, Spain: Tectonics, v. 14, p. 1368–1379, doi:10.1029/95TC01976.
Hossack, J.R., 1979, The use of balanced cross-sections in the calculation of orogenic contraction: A review: Journal of the Geological Society of London, v. 136, no. 6, p. 705–711, doi:10.1144/gsjgs.136.6.0705.
Hunter, R.B., 1987, Timing and structural relations between the Gros Ventre foreland uplift, the Prospect thrust system and the Granite Creek thrust, Hoback Basin, Wyoming, *in* Miller, W.R., ed., Wyoming Geological Association Guidebook, p. 109–131.
Hunter, R.B., 1988, Timing and structural interaction between the thrust belt and foreland, Hoback Basin, Wyoming, *in* Schmidt, C.J., and Perry, W.J., eds., Interaction of the Rocky Mountain Foreland and the Cordilleran Thrust Belt: Geological Society of America Memoir 171, p. 431–445.
Ismat, Z., and Mitra, G., 2005a, Fold-thrust belt evolution expressed in an internal thrust sheet, Sevier orogeny: The role of cataclastic flow: Geological Society of America Bulletin, v. 117, p. 764–782, doi:10.1130/B25514.1.
Ismat, Z., and Mitra, G., 2005b, Folding by cataclastic flow: Evolution of controlling factors during deformation: Journal of Structural Geology, v. 27, p. 2181–2203, doi:10.1016/j.jsg.2005.08.005.
Jordan, T.E., 1981, Thrust loads and foreland basin evolution, Cretaceous, western U.S.: American Association of Petroleum Geologists Bulletin, v. 65, p. 2506–2520.
Kempf, O., Schlunegger, F., Strunck, P., and Matter, A., 1998, Palaeomagnetic evidence for late Miocene rotation of the Swiss Alps: Results from the north Alpine foreland basin: Terra Nova, v. 10, no. 1, p. 6–10, doi:10.1046/j.1365-3121.1998.00164.x.
Kent, D.V., 1988, Further paleomagnetic evidence for oroclinal rotation in the central folded Appalachians from the Bloomsburg and Mauch Chunk Formations: Tectonics, v. 7, p. 749–759, doi:10.1029/TC007i004p00749.
Kley, J., and Monaldi, C.R., 1998, Tectonic shortening and crustal thickness in the Central Andes: How good is the correlation?: Geology, v. 26, no. 8, p. 723–726, doi:10.1130/0091-7613(1998)026<0723:TSACTI>2.3.CO;2.
Kodama, K.P., 1988, Remanence rotation due to rock strain during folding and the stepwise application of the fold test: Journal of Geophysical Research, ser. B, Solid Earth and Planets, v. 93, no. B4, p. 3357–3371, doi:10.1029/JB093iB04p03357.
Kollmeier, J.M., van der Pluijm, B.A., and Van der Voo, R., 2000, Analysis of Variscan dynamics: Early bending of the Cantabria-Asturias Arc, northern Spain: Earth and Planetary Science Letters, v. 181, no. 1–2, p. 203–216.
Kwon, S., and Mitra, G., 2004, Strain distribution, strain history, and kinematic evolution associated with the formation of arcuate salients in fold-thrust belts: The example of the Provo salient, Sevier orogen, Utah, *in* Sussman A.J., and Weil A.B., eds., Orogenic Curvature—Integrating Paleomagnetic and Structural Analyses: Geological Society of America Special Paper 383, p. 205–223.
Lawton, T.F., Boyer, S.E., and Schmidt, J.G., 1994, Influence of inherited taper on structural variability and conglomerate distribution, Cordilleran fold and thrust belt, western United States: Geology, v. 22, p. 339–342, doi:10.1130/0091-7613(1994)022<0339:IOITOS>2.3.CO;2.
Lowrie, W., Hirt, A.M., and Kligfield, R., 1986, Effects of tectonic deformation on the remanent magnetization of rocks: Tectonics, v. 5, no. 5, p. 713–722, doi:10.1029/TC005i005p00713.
Mattei, M., Petrocelli, V., Lacava, D., and Schiattarella, M., 2004, Geodynamic implications of Pleistocene ultrarapid vertical-axis rotations in the Southern Apennines, Italy: Geology, v. 32, no. 9, p. 789–792, doi: 10.1130/G20552.1
McKenzie, D.P., and Jackson, J.A., 1983, The relationship between strain rates, crustal thickening, paleomagnetism, finite strain, and fault movement within a deforming zone: Earth and Planetary Science Letters, v. 65, p. 182–202, doi:10.1016/0012-821X(83)90198-X.
McNaught, M.A., and Mitra, G., 1996, The use of finite strain data in constructing retrodeformable balanced cross-sections, Meade thrust sheet, Idaho, U.S.A., *in* McClay, K.R., ed., Thrust Tectonics 1990 Abstracts: London, Royal Holloway and Bedford New College, University of London, p. 30.
McWhinnie, S.T., van de Pluijm, B.A., and Van der Voo, R., 1990, Remagnetizations and thrusting in the Idaho-Wyoming Overthrust belt: Journal of Geophysical Research, v. 95, no. B4, p. 4551–4559, doi:10.1029/JB095iB04p04551.
Means, W.D., 1976, Stress and Strain: New York, Springer-Verlag, 339 p.
Millán, H., Pocoví, A., and Casas, A., 1995, El frente de cabalgamiento surpirenaico en el extremo occidental de las Sierras Exteriores: Sistemas imbricados y pliegues de despegue: Revista de la Sociedad Geológica de España, v. 8 no. 1–2, p. 73–90.
Millán, H., Pueyo, E.L., Aurell, M., Luzón, A., Oliva, B., Martínez-Peña, M.B., and Pocoví, A., 2000, Actividad tectónica registrada en los depósitos terciarios del frente meridional del Pirineo central: Revista de la Sociedad Geológica de España, v. 13, no. 2, p. 279–300.
Mitra, G., 1994, Strain variation in thrust sheets across the Sevier fold-and-thrust belt (Idaho-Utah-Wyoming): Implications for section restoration and wedge taper evolution: Journal of Structural Geology, v. 16, no. 4, p. 585–602, doi:10.1016/0191-8141(94)90099-X.
Mochales, T., Casas, A.M., Pueyo, E.L., and Barnolas, A., 2012, Rotational velocity for oblique structures (Boltaña anticline, southern Pyrenees): Journal of Structural Geology, v. 35, p. 2–16, doi:10.1016/j.jsg.2011.11.009.
Moretti, I., 2008, Working in complex areas: New restoration workflow based on quality control, 2D and 3D restorations: Marine and Petroleum Geology, v. 25, p. 205–218, doi:10.1016/j.marpetgeo.2007.07.001.
Moretti, I., Lepage, F., and Guiton, M., 2005, KINE3D: A new 3D restoration method based on a mixed approach linking geometry and geomechanics: Oil & Gas Science and Technology, v. 60, p. 1–12.
Mukul, M., and Mitra, G., 1998, Finite strain and strain variation analysis in the Sheeprock thrust sheet: An internal thrust sheet in the Provo salient of the Sevier fold-and-thrust belt, central Utah: Journal of Structural Geology, v. 20, no. 4, p. 385–405, doi:10.1016/S0191-8141(97)00087-4.

Muron, P., Mallet, J.-L., and Medwedeff, D., 2005, 3D sequential structural restoration: Geometry and kinematics, *in* 2005 American Association of Petroleum Geologists Annual Convention: Calgary, Canada, American Association of Petroleum Geologists.

Norris, D.K., and Black, R.F., 1961, Application of palaeomagnetism to thrust mechanics: Nature, v. 192, no. 4806, p. 933–935, doi:10.1038/192933a0.

Oldow, J.S., Channell, J.E.T., Catalano, R., and D'Argenio, B., 1990, Thrusting and large-scale rotations in the western Sicilian fold and thrust belt: Tectonics, v. 9, no. 4, p. 661–682, doi:10.1029/TC009i004p00661.

Oliva-Urcia, B., and Pueyo, E.L., 2007, Gradient of shortening and vertical-axis rotations in the Southern Pyrenees (Spain), insights from a synthesis of paleomagnetic data: Revista de la Sociedad Geológica de España, v. 20, no. 1–2, p. 105–118.

Oliva-Urcia, B., Pueyo, E.L., and Larrasoaña, J.C., 2008, Magnetic reorientation induced by pressure solution: A potential mechanism for orogenic-scale remagnetizations: Earth and Planetary Science Letters, v. 265, p. 525–534, doi:10.1016/j.epsl.2007.10.032.

Oliva, B., Casas, A.M., Pueyo, E.L., Pocoví, A., 2012, Structural and paleomagnetic evidence for non-rotational kinematics in the western termination of the External Sierras (southwestern central Pyrenees): Geologica Acta, v. 10, no. 1, p. 125–144.

Onderdonk, N.W., Minor, S.A., and Kellogg, K.S., 2005, Taking apart the Big Pine fault: Redefining a major structural feature in southern California: Tectonics, v. 24, 11 p., doi:10.1029/2005TC001817.

Price, R.A., 1981, The Cordilleran foreland thrust and fold belt in the southern Canadian Rocky Mountains: Geological Society of London Special Publication 9, p. 427–448, doi:10.1144/GSL.SP.1981.009.01.39.

Protzman, G.M., and Mitra, G., 1990, Strain fabrics associated with the Meade thrust: Implications for cross-section balancing: Journal of Structural Geology, v. 12, p. 403–417, doi:10.1016/0191-8141(90)90030-3.

Pueyo, E.L., 2000, Rotaciones paleomagnéticas en sistemas de pliegues y cabalgamientos: Tipos, causas, significado y aplicaciones (ejemplos de las Sierras Exteriores y de la Cuenca de Jaca, Pirineo Aragonés) [Ph.D. thesis]: Zaragoza, Spain, Universidad de Zaragoza, 296 p.

Pueyo, E.L., 2010, Evaluating the paleomagnetic reliability in fold and thrust belt studies: Trabajos de Geologia, v. 30, no. 1, p. 145–154.

Pueyo, E.L., Millán, H., Pocoví, A., and Parés, J.M., 1997, Cinemática rotacional del cabalgamiento basal surpirenaico en las Sierras Exteriores Aragonesas: Datos magnetotectónicos: Acta Geológica Hispánica, v. 32, no. 3–4, p. 119–138.

Pueyo, E.L., Millán, H., and Pocoví, A., 2002, Rotation velocity of a thrust: A paleomagnetic study in the External Sierras (Southern Pyrenees), *in* Marzo, M., Muñoz, J.A., and Vergés, J., eds., Growth Strata: Sedimentary Geology, v. 146, p. 191–208, doi: 10.1016/S0037-0738(01)00172-5.

Pueyo E.L., Parés, J.M., Millán, H., and Pocoví, A., 2003a, Conical folds and apparent rotations in paleomagnetism (A case study in the Pyrenees): Tectonophysics, v. 362, no. 1–4, p. 345–366.

Pueyo, E.L., Pocoví, A., Parés, J.M., Millán, H., and Larrasoaña, J.C., 2003b, Thrust ramp geometry and spurious rotations of paleomagnetic vectors: Studia Geophysica et Geodaetica, v. 47, p. 331–357, doi:10.1023/A:1023775725268.

Pueyo, E.L., Pocoví, A., Millán, H., and Sussman, A., 2004, Map-view models for correcting and calculating shortening estimates in rotated thrust fronts using paleomagnetic data, *in* Sussman, A.J., and Weil, A.B., eds., Orogenic Curvature: Integrating Paleomagnetic and Structural Analyses: Geological Society of America Special Paper 383, p. 57–71.

Pueyo, E.L., Mauritsch, H.J., Gawlick, H.J., Scholger, R., and Frisch, W., 2007, New evidence for block and thrust sheet rotations in the central northern Calcareous Alps deduced from two pervasive remagnetization events: Tectonics, v. 26, TC5011, 25 p.

Pueyo-Anchuela, O., Pueyo, E.L., Pocoví, A., Gil-Imaz, A., 2012, Vertical axis rotations in thrust and folds belts: Calibration of AMS and paleomagnetic data in the Western External Sierras (Southern Pyrenees): Tectonophysics, v. 532–535, p. 119–133, doi:10.1016/j.tecto.2012.01.023

Ramón, M.J., Pueyo, E.L., Briz, J.L., Pocoví, A., and Ciria, J.C., 2012, Flexural unfolding in 3D using paleomagnetic vectors: Journal of Structural Geology, v. 35; p. 28–39, doi:10.1016/j.jsg.2011.11.015.

Ramsay, J.G., 1967, Folding and Fracturing of Rocks: New York, McGraw Hill, 568 p.

Ramsay, J.G., 1976, Displacement and strain: Philosophical Transactions of the Royal Society of London, v. 283, no. 1312, p. 3–25.

Rodríguez-Pintó, A., Ramón, M.J., Oliva-Urcia, B., Pueyo, E.L., and Pocoví, A., 2011, Errors in paleomagnetism: Structural control on overlapped vectors, mathematical models: Physics of the Earth and Planetary Interiors, v. 186, p. 11–22, doi:10.3166/ga.23.151-165.

Ron, H., Freund, R., and Garfunkel, Z., 1984, Block rotation by strike-slip faulting: Structural and paleomagnetic evidence: Journal of Geophysical Research, v. 89, p. 6256–6270, doi:10.1029/JB089iB07p06256.

Roperch, P., Fornari, M., Hérail, G., and Parraguez, G.V., 2000, Tectonic rotations within the Bolivian Altiplano: Implications for the geodynamic evolution of the Central Andes during the Late Tertiary: Journal of Geophysical Research, v. 105, p. 795–820.

Rouby, D., Suppe, J., and Xiao, H., 2000, 3D restoration of complexly faulted and folded surfaces using multiple unfolding mechanisms: American Association of Petroleum Geologists Bulletin, v. 84, p. 805–829.

Royse, F., 1993, Case of the Phantom foredeep: Early Cretaceous in west-central: Utah Geology, v. 21, p. 133–136, doi:10.1130/0091-7613(1993)021<0133:COTPFE>2.3.CO;2.

Royse, F., Warner, M.A., and Reese, D.L., 1975, Thrust belt structural geometry and related stratigraphic problems, Wyoming–Idaho–northern Utah: Rocky Mountain Association of Geologists Symposium, p. 41–45.

Rumelhart, P.E., Yin, A., Cowgill, E., Butler, R., Zhang, Q., and Wang, X.F., 1999, Cenozoic vertical-axis rotation of the Altyn Tagh fault system: Geology, v. 27, p. 819–822, doi:10.1130/0091-7613(1999)027<0819:CVAROT>2.3.CO;2.

Schwartz, S.Y., and Van der Voo, R., 1984, Paleomagnetic study of thrust sheet rotation during foreland impingement in the Wyoming–Idaho Overthrust belt: Journal of Geophysical Research, v. 89, p. 10,077–10,086, doi:10.1029/JB089iB12p10077.

Smith, R.B., and Bruhn, R.L., 1984, Intraplate extensional tectonics of the eastern Basin-Range: Inferences on structural style from seismic reflection data, regional tectonics, and thermal-mechanical models of brittle-ductile deformation: Journal of Geophysical Research, v. 89, no. B7, p. 5733–5762, doi:10.1029/JB089iB07p05733.

Soto, R., Casas, A.M., and Pueyo, E.L., 2006, Along-strike variation of orogenic wedges associated with vertical axis rotations: Journal of Geophysical Research, v. 111, B10402, doi:10.1029/2005JB004201.

Stamatakos, J., and Hirt, A.M., 1994, Paleomagnetic considerations of the development of the Pennsylvania salient in the central Appalachians: Tectonophysics, v. 231, p. 237–255, doi:10.1016/0040-1951(94)90037-X.

Stewart, S.A., 1995, Paleomagnetic analysis of plunging fold structures: Errors and a simple fold test: Earth and Planetary Science Letters, p. 130, p. 57–67.

Sussman, A.J., Butler, R.F., Dinares-Turell, J., and Verges, J., 2003, Vertical-axis rotation of a foreland fold and implications for orogenic curvature: An example from the Southern Pyrenees, Spain: Earth and Planetary Science Letters, v. 218, p. 435–449, doi:10.1016/S0012-821X(03)00644-7.

Thibert, B., Gratier, J.P., and Morvan, J.M., 2005, A direct method for modeling and unfolding developable surfaces and its application to the Ventura Basin (California): Journal of Structural Geology, v. 27, p. 303–316, doi:10.1016/j.jsg.2004.08.011.

Thöny, W., Ortner, H., and Scholger, R., 2006, Paleomagnetic evidence for large en-bloc rotations in the eastern Alps during Neogene orogeny: Tectonophysics, v. 414, no. 1–4, p. 169–189, doi:10.1016/j.tecto.2005.10.021.

van der Pluijm, B.A., 1987, Grain scale deformation and the fold test-evaluation of synfolding remagnetization: Geophysical Research Letters, v. 14, p. 155–157, doi:10.1029/GL014i002p00155.

Van der Voo, R., 1990, The reliability of paleomagnetic data: Tectonophysics, v. 184, p. 1–9, doi:10.1016/0040-1951(90)90116-P.

Van der Voo, R., Stamatakos, J.A., and Parés, J.M., 1997, Kinematic constraints on thrust-belt curvature from syndeformational magnetizations in the Lagos del Valle syncline in the Catabrian Arc, Spain: Journal of Geophysical Research, v. 102, no. B5, p. 10,105–10,119, doi:10.1029/97JB00263.

Von Winterfeld, C., and Oncken, O., 1995, Non-plane strain in section balancing: Calculation of restoration parameters: Journal of Structural Geology, v. 17, no. 3, p. 447–450, doi:10.1016/0191-8141(94)00086-F.

Weil, A.B., 2006, Kinematics of orocline tightening in the core of an arc: Paleomagnetic analysis of the Ponga Unit, Cantabria Arc, northern Spain: Tectonics, v. 25, 2005TC001861, p. 1–23.

Weil, A.B., and Sussman, A.J., 2004, Classifying curved orogens based on timing relationships between structural development and vertical-axis rotations, *in* Sussman, A.J., and Weil, A.B., eds., Orogenic Curvature: Integrating Paleomagnetic and Structural Analyses: Geological Society of America Special Paper 383, p. 1–15.

Weil, A.B., and Van der Voo, R., 2002, The evolution of the paleomagnetic fold test as applied to complex geologic situations, illustrated by a case study from northern Spain: Physics and Chemistry of the Earth, v. 27, p. 1223–1235.

Weil, A.B., Van der Voo, R., van der Pluijm, B.A., and Pares, J., 2000, The formation of an orocline by multiphase deformation: A paleomagnetic investigation of the Cantabria-Asturias Arc (northern Spain): Journal of Structural Geology, v. 22, no. 6, p. 735–756, doi:10.1016/S0191-8141(99)00188-1.

Weil, A.B., Van der Voo, R., and van der Pluijm, B., 2001, New paleomagnetic data from the southern Cantabria-Asturias Arc, northern Spain: Implications for true oroclinal rotation and the final amalgamation of Pangea: Geology, v. 29, p. 991–994.

Weil, A.B., Yonkee, A.W., and Sussman, A.J., 2010, Reconstructing the kinematic evolution of curved mountain belts: A paleomagnetic study of Triassic red beds from the Wyoming salient, Sevier thrust belt: Geological Society of America Bulletin, v. 122, p. 3–23, doi:10.1130/B26483.1.

Wilkerson, M.S., 1992, Differential transport and continuity of thrust sheets: Journal of Structural Geology, v. 14, no. 6, p. 749–751, doi:10.1016/0191-8141(92)90132-G.

Williams, G.D., Kane, S., Buddin, T.S., and Richards, A.J., 1997, Restoration and balance of complex folded and faulted rock volumes: Flexural flattening, jigsaw fitting and decompaction in three dimensions: Tectonophysics, v. 273, no. 3–4, p. 203–218.

Wiltschko, D.V., and Dorr, J.A., 1983, Timing of deformation in overthrust belt and foreland of Idaho, Wyoming and Utah: The American Association of Petroleum Geologists Bulletin, v. 67, p. 1304–1322.

Woodward, N.B., Gray, D.R., and Spears, D.B., 1986, Including strain data in balanced cross-sections, *in* Platt, J.P., Coward, M.P., Deramond, J., and Hossack, J., eds., Thrusting and Deformation: Journal of Structural Geology, v. 8, no. 3–4, p. 313–324.

Woodward, N.B., Boyer, S.E., and Suppe, J., 1989, Balanced geological cross sections: An essential technique in geologic research and exploration, *in* 28th International Geological Congress: Washington, D.C., American Geophysical Union, Short Course in Geology, v. 6, 132 p.

Yonkee, A., Weil, A.B., 2010, Reconstructing the kinematic evolution of curved mountain belts: Internal strain patterns in the Wyoming Salient, Sevier thrust belt, U.S.A.: Geological Society of America Bulletin, v. 122, p. 24–49.

MANUSCRIPT RECEIVED 6 SEPTEMBER 2011
REVISED MANUSCRIPT RECEIVED 2 MARCH 2012
MANUSCRIPT ACCEPTED 6 MARCH 2012

Printed in the USA